Electronic Supplementary Material (ESI) for Nanoscale.
This journal is © The Royal Society of Chemistry 2015

Supplementary Information

Surface-modified piezoresistive nanocomposite flexible pressure sensors with high sensitivity and wide linearity

Yi Shu,[ab] *He Tian,*[ab] *Yi Yang,*[ab] *Cheng Li,*[ab] *Yalong Cui,*[ab] *Wentian Mi,*[ab] *Yuxing Li,*[ab] *Zhe Wang,*[ab] *Ningqin Deng,*[ab] *Bo Peng*[ab] *and Tian-Ling Ren*[ab]*

a Institute of Microelectronics, Tsinghua University, Beijing 100084, China. E-mail: RenTL@tsinghua.edu.cn
b Tsinghua National Laboratory for Information Science and Technology (TNList), Tsinghua University, Beijing 100084, China

The surface measurement results of the samples with roughness grade P200 P400 P800 and P1200

a

P200

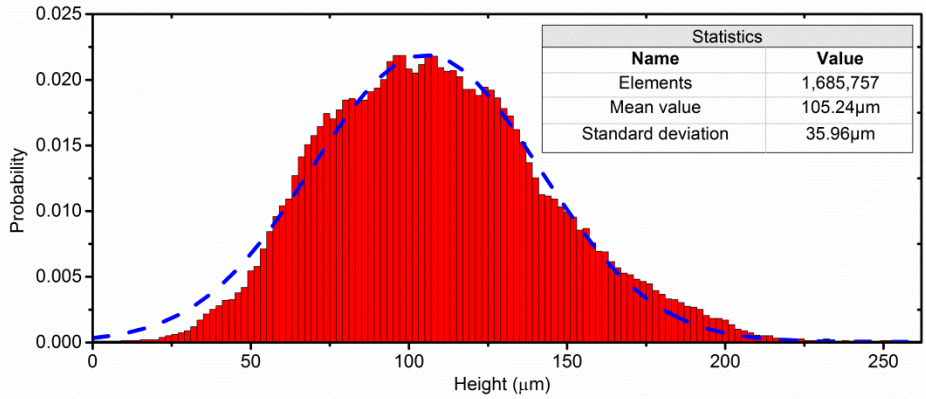

P400

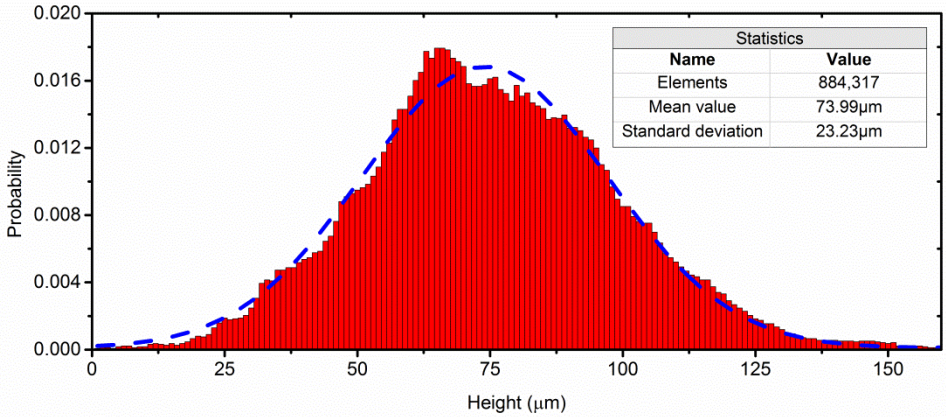

P800

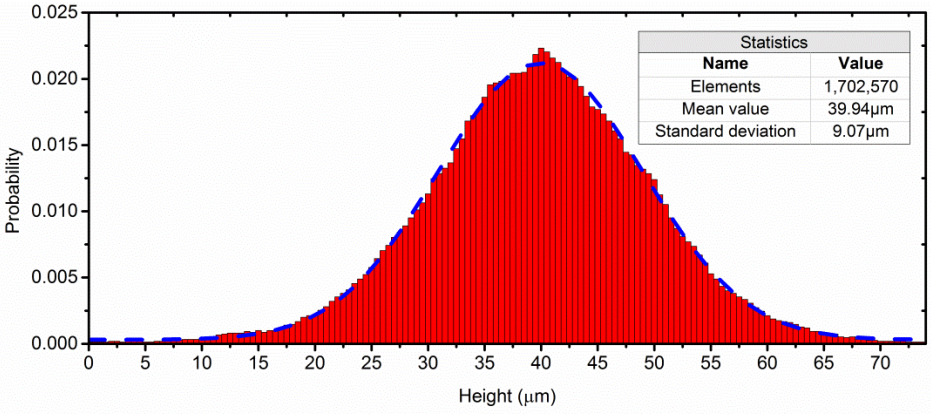

P1200

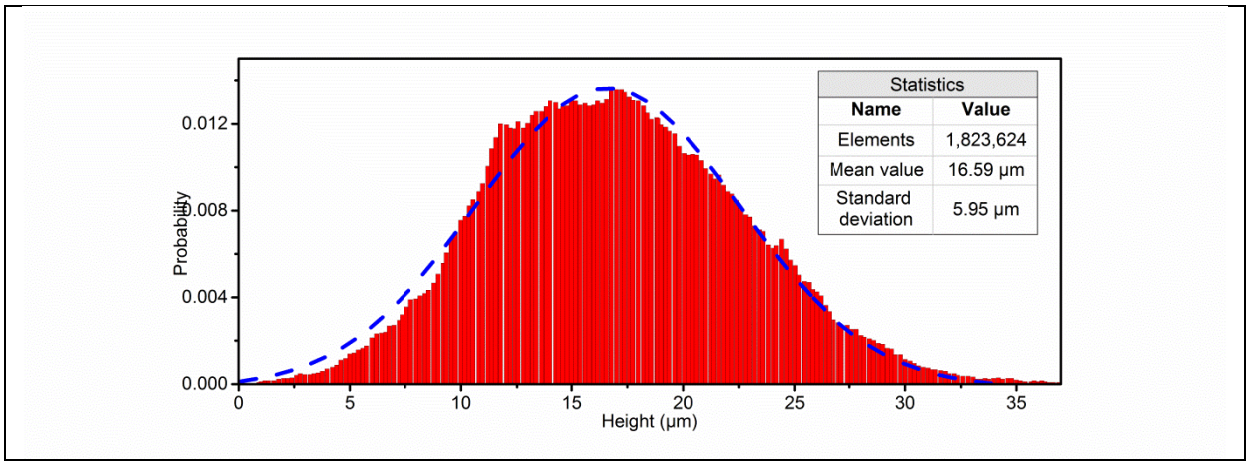

b

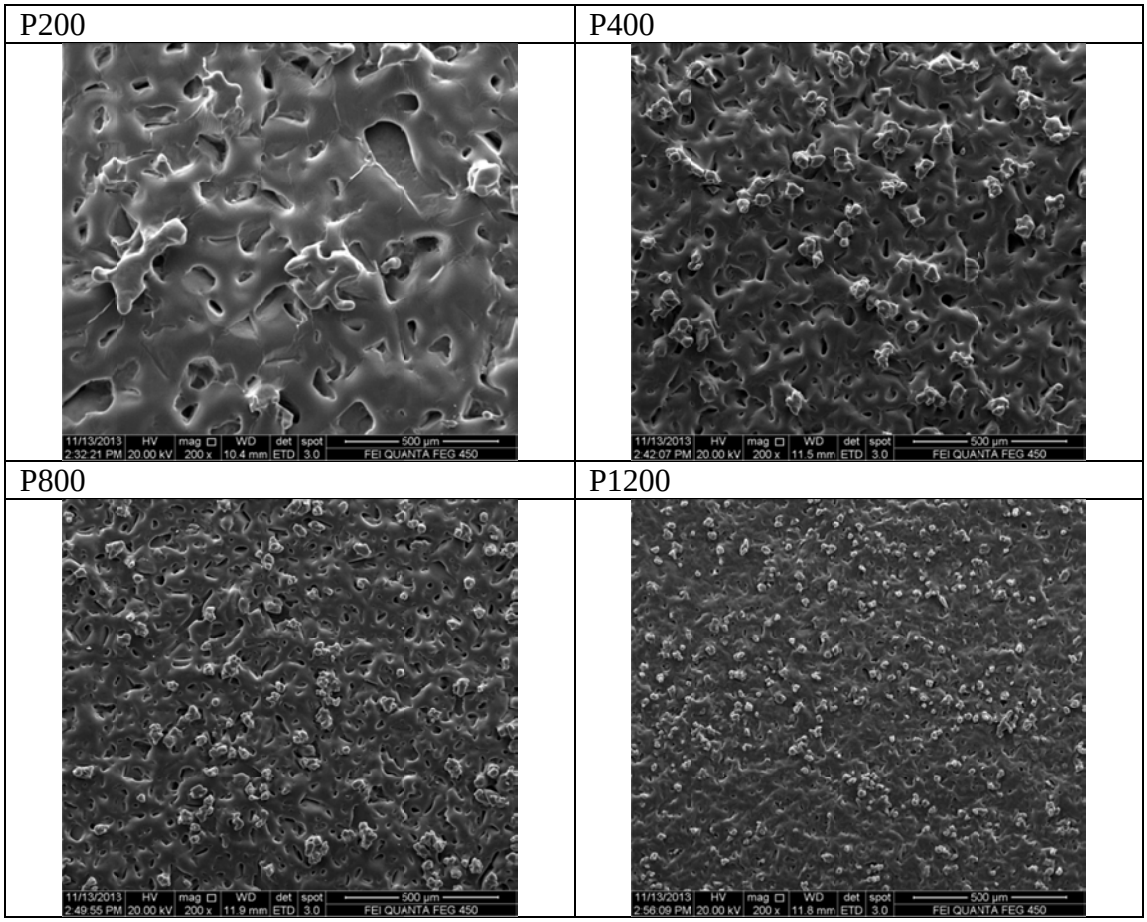

Supplementary Figure S1 (a) The measured height distribution of the samples with mould grade P200, P400, P800 respectively; (b) The SEM photos of the corresponding samples.

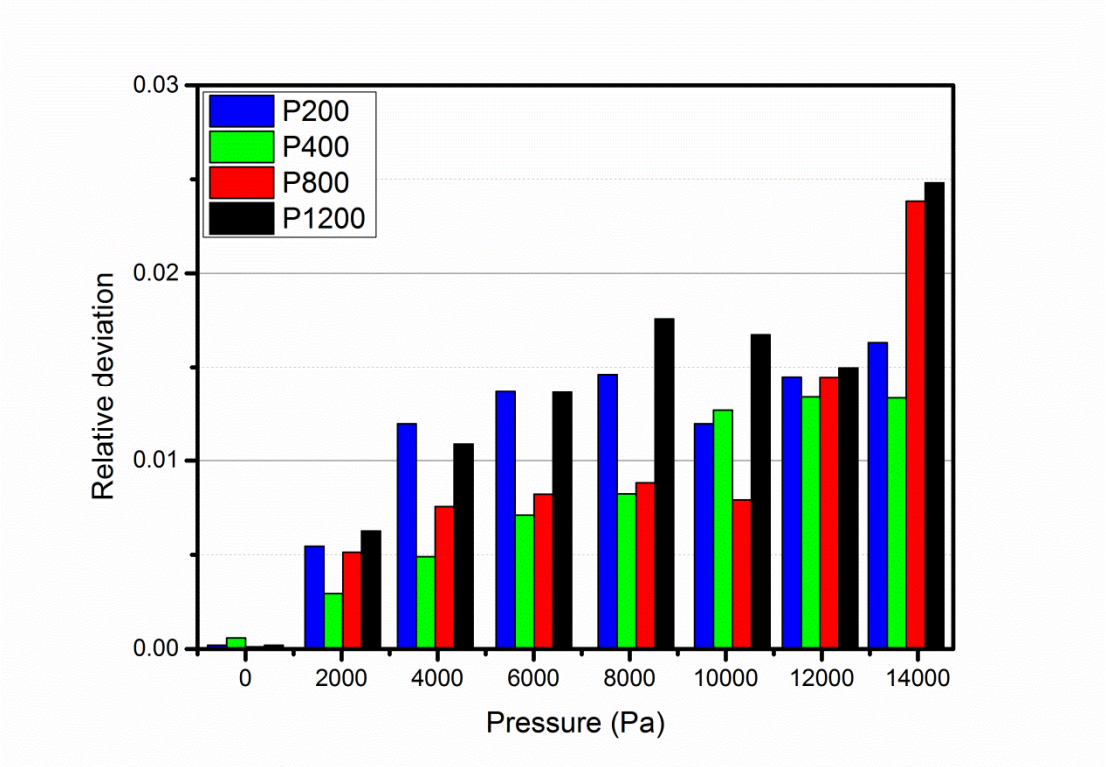

Supplementary Figure S2 demonstrates the Relative deviation of four samples at different pressure levels, calculated by the division of the standard deviation by full scale measured value. The relative deviation can be worked out which are no more than 2.5% all along the working scale.

Frequency response of the Device

f=1Hz

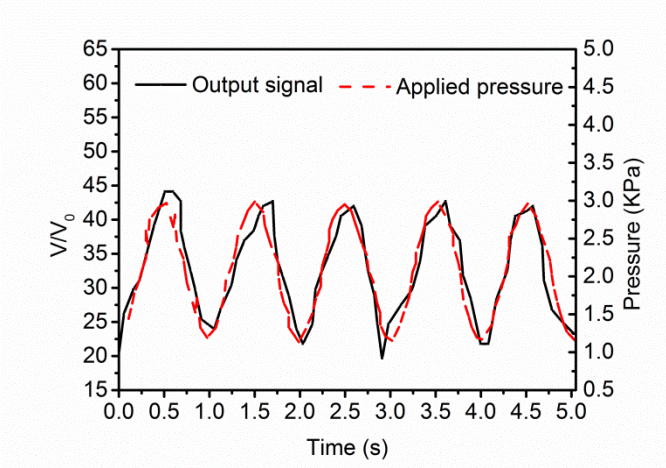

f=4.55Hz

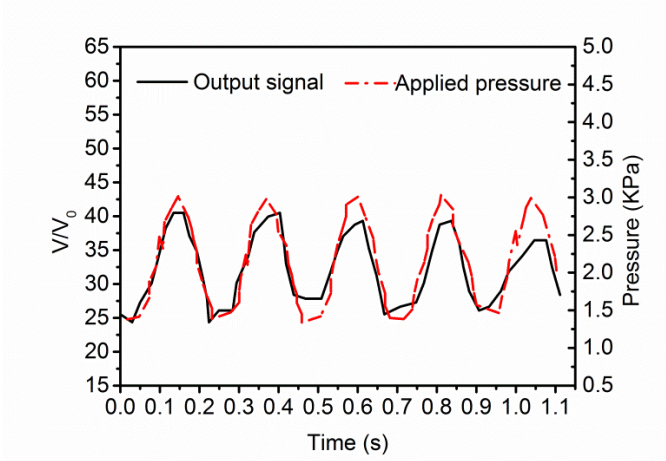

f=19.2Hz

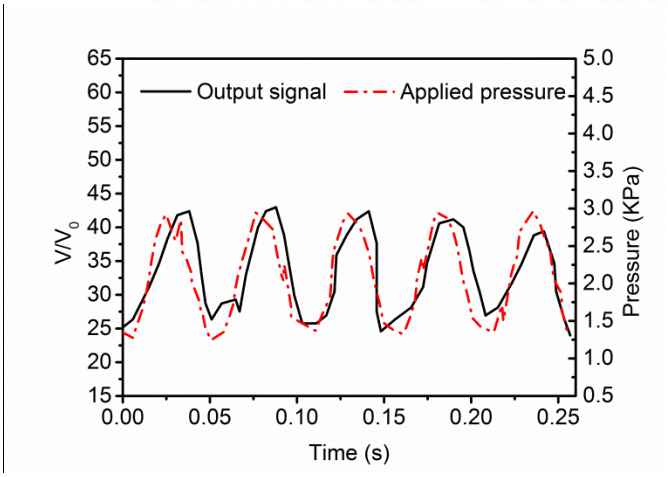

Supplementary Figure S3 demonstrates the frequency response with the loading frequency 1Hz, 4.55Hz, 19.2 Hz respectively. The applied pressure wave and the response signals remain synchronous at low frequencies until the frequency reaches to almost 20Hz, an obvious delay of the output signals can be observed.

The equivalent circuit, physical image and equations used in the simulation

a

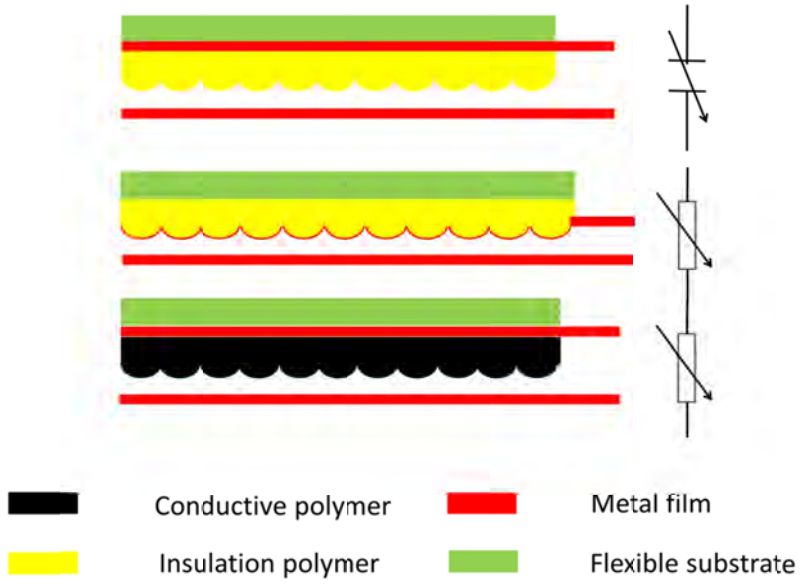

b

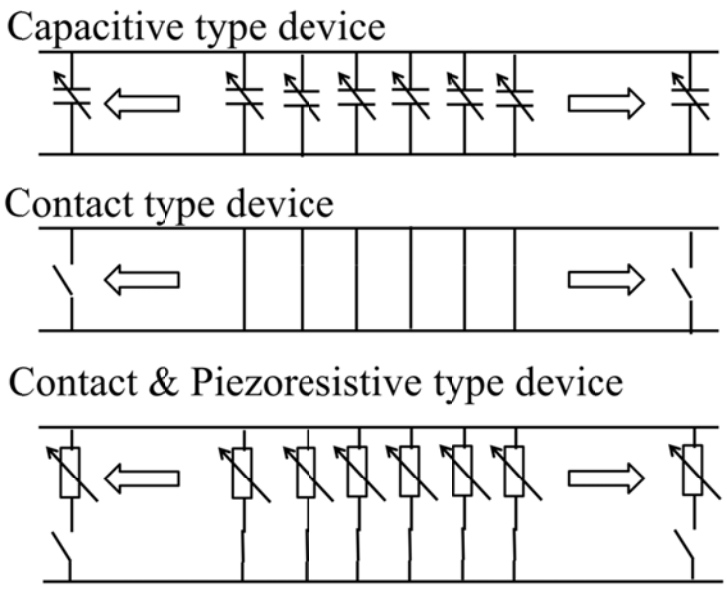

c

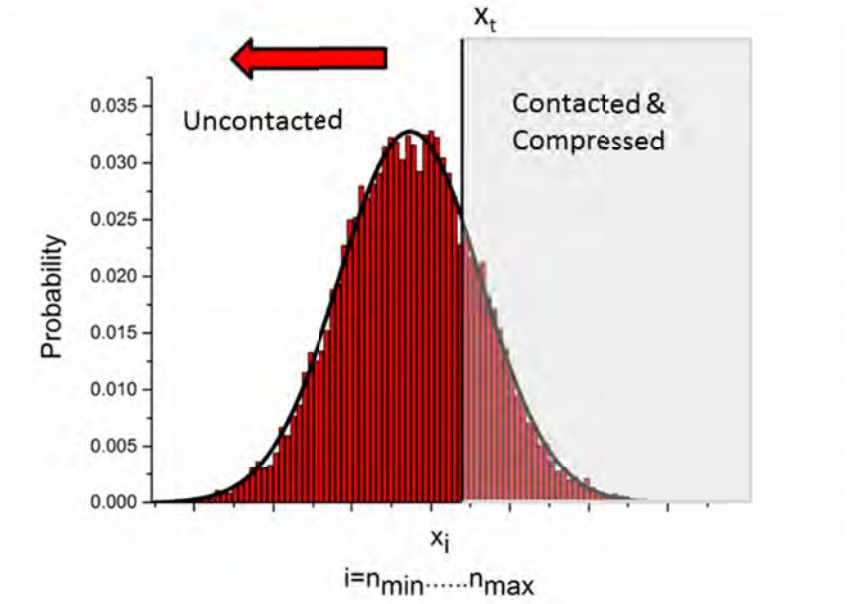

d

Capacitive type device

$$P(x_i) = S * \sum_{i=t}^{n_{max}} [DF(x_i + \Delta x_i) - DF(x_i)] * p\left(\frac{x_i - x_t}{x_i}\right)$$

$$Ca(x_i) = S * \sum_{i=t}^{n_{max}} [DF(x_i + \Delta x_i) - DF(x_i)] * \frac{\varepsilon_0 \varepsilon_p}{x_t}$$

$$+S * \sum_{i=n_{min}}^{t-1} [DF(x_i + \Delta x_i) - DF(x_i)] * [\frac{1}{\frac{x_i}{\varepsilon_0 \varepsilon_p} + \frac{x_t - x_i}{\varepsilon_0}}]$$

Contact type device

$$P(x_i) = S * \sum_{i=t}^{n_{max}} [DF(x_i + \Delta x_i) - DF(x_i)] * p\left(\frac{x_i - x_t}{x_i}\right)$$

$$Co(x_i) = S * \sum_{i=t}^{n_{max}} [DF(x_i + \Delta x_i) - DF(x_i)]$$

Contact & Piezoresistive type device

$$P(x_i) = S * \sum_{i=t}^{n_{max}} [DF(x_i + \Delta x_i) - DF(x_i)] * p\left(\frac{x_i - x_t}{x_i}\right)$$

$$Cond(x_i) = S * \sum_{i=t}^{n_{max}} [DF(x_i + \Delta x_i) - DF(x_i)] * \frac{1}{x_i} * cond(\frac{x_i - x_t}{x_i})$$

Supplementary Figure S5 (a) Three different working principles of the pressure sensor; (b) Equivalent circuits of three different working principles of the flexible pressure sensor; (c) Demonstration of a general physical picture (Take Gauss distribution as an example) when the micro structures are compressed to the height of x_t, all the portions with the height higher

than x_t are compressed to the height of x_t with different strain degree depending on their original height, other portions remain original state; (d) The numerical models of these three different working principles.

The meanings of the symbols in these equations are listed below:

DF-Distribution functions of the micro-structured profile;

P-Pressure applied on the device

Ca-Capacitance of the device

Co-Contact ration of the device

Cond-Conductivity of the device

p-bulk polymer materials' strain-stress property

cond- bulk conductive polymer materials' piezoresistive property

Demonstrations of 9 different profile models

Pyramid-1Dimension	Pyramid-2Dimension
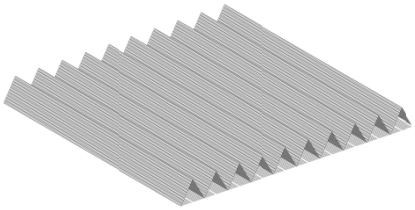	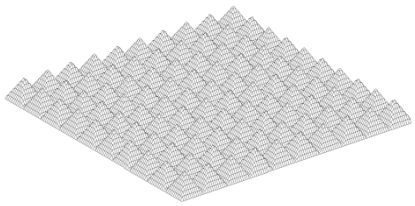
Brick-1Dimension	Brick-2Dimension
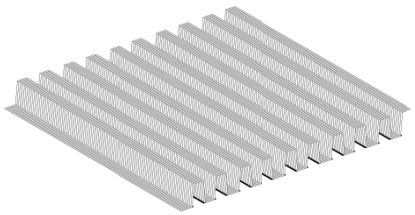	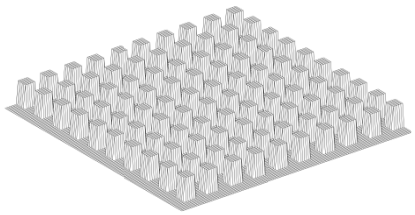
Sine-1Dimension	Sine-2Dimension
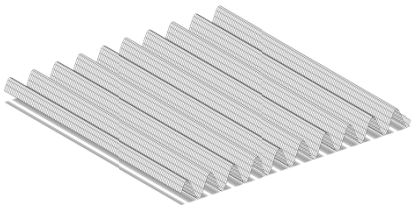	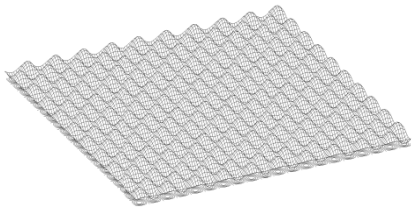
Sphere-1Dimension	Sphere-2Dimension
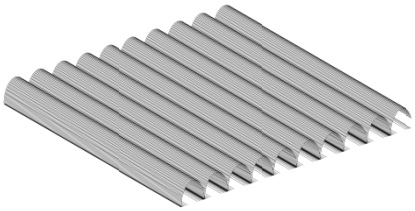	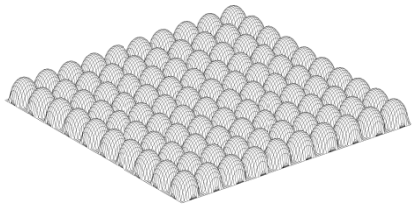
Gauss random distribution rough surface	
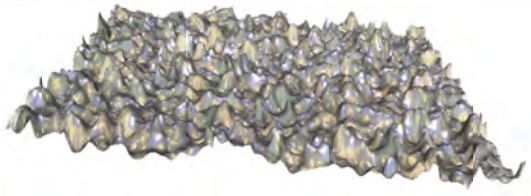	

Supplementary Figure S6 Demonstrations of 9 different profile models. **T**he Pyramid & Sphere structures have no gaps between them. The Sine wave-like surface profile obeys the Sinusoidal function. The two Brick structures' profile has the duty cycle of 1:1.

The height distribution of different surface profiles

Pyramid-1D	Pyramid-2D	Brick-1D
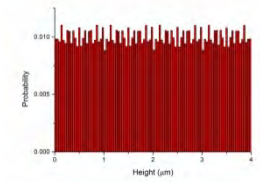	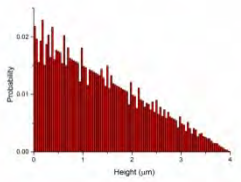	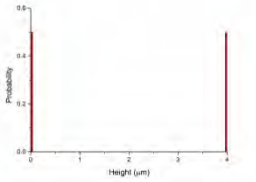
Brick-2D	**Sine-1D**	**Sine-2D**
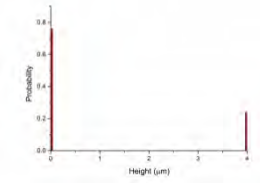	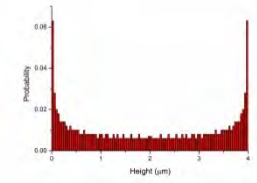	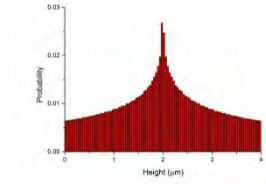
Sphere-1D	**Sphere-2D**	**Random rough surface**
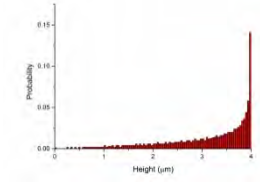	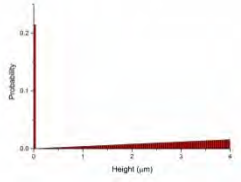	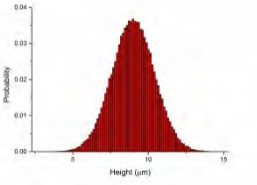

Supplementary Figure S7 The height distribution of different surface profiles

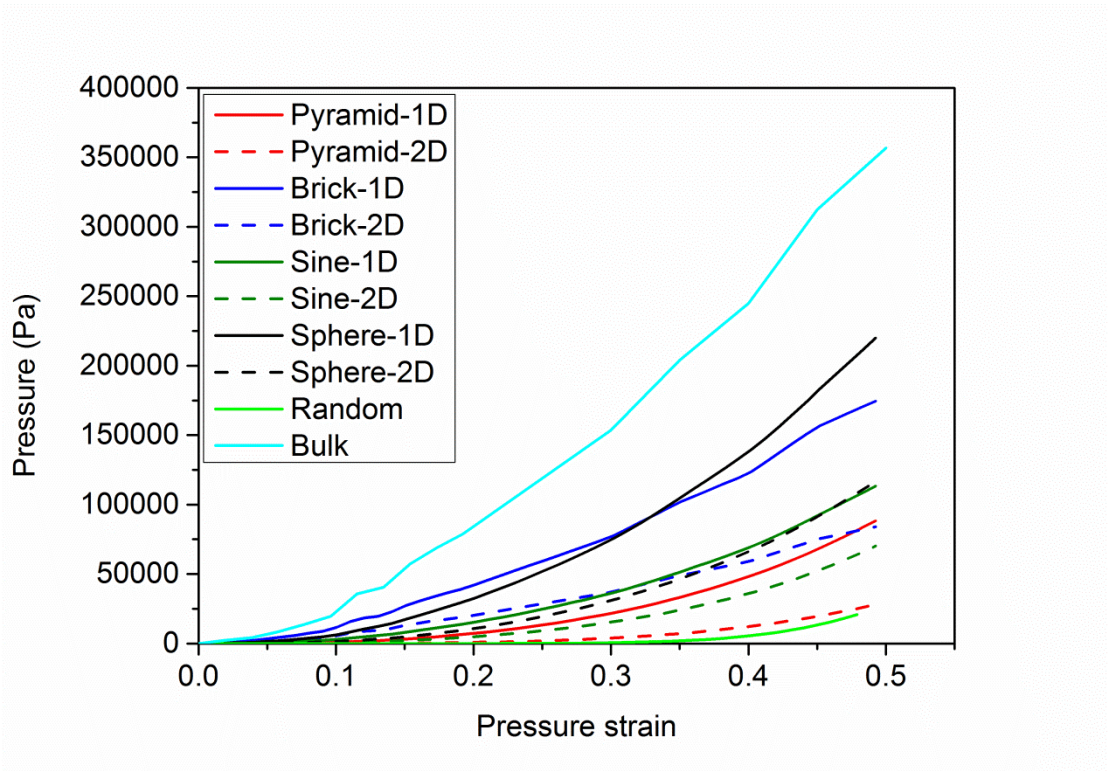

Supplementary Figure S8 The elastic responds of the different surface profiles

Two layer device structures and their height distributions at different sliding steps

a

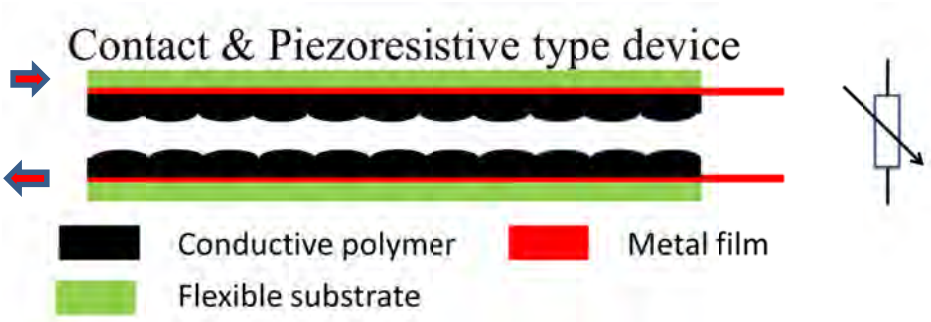

b

	Pyramid-1D	Pyramid-2D	Brick-1D
Original state	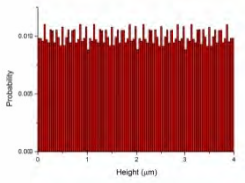	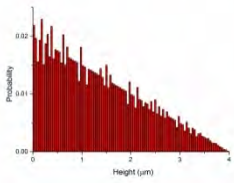	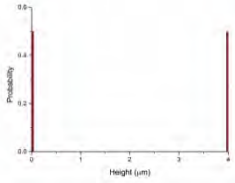
1st shift step	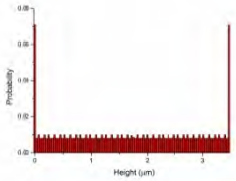	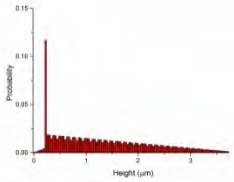	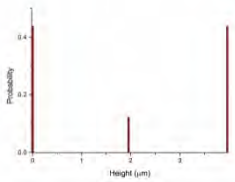
2nd shift step	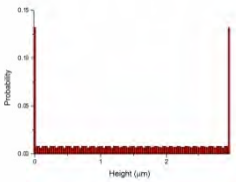	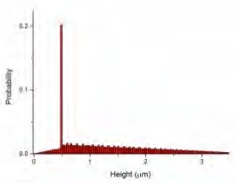	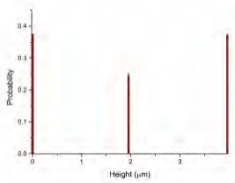
3rd shift step	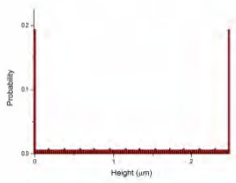	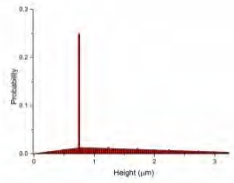	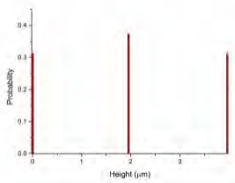
4th shift step	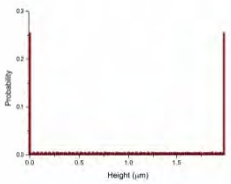	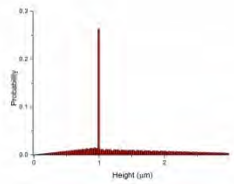	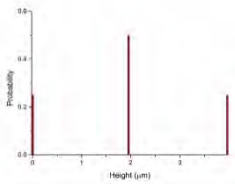

	Brick-2D	Sine-1D	Sine-2D
Original state	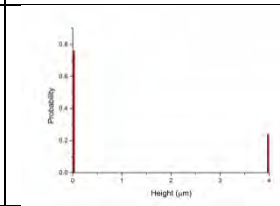	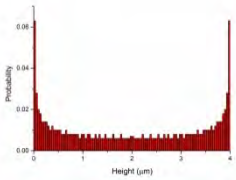	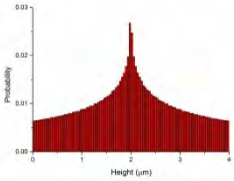
1st shift step	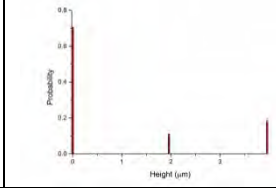	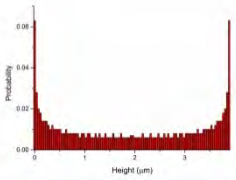	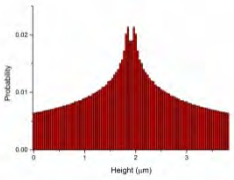
2nd shift step	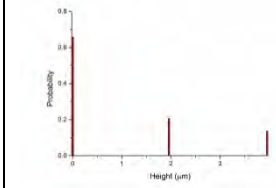	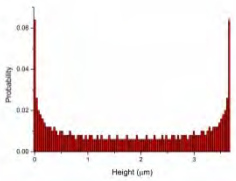	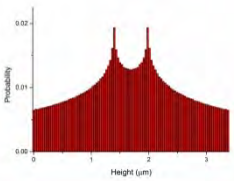
3rd shift step	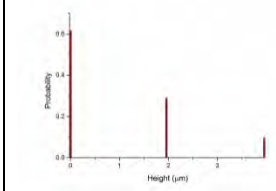	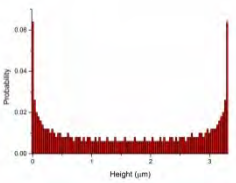	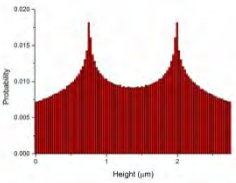
4th shift step	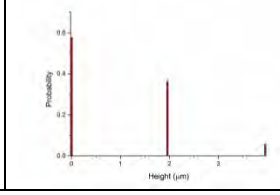	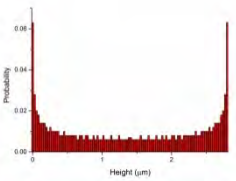	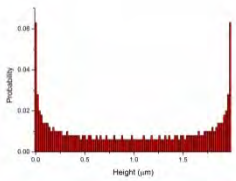

	Sphere-1D	Sphere-2D	Random rough surface
Original state	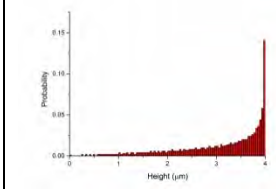	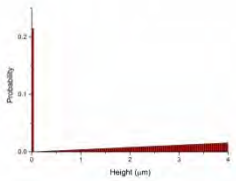	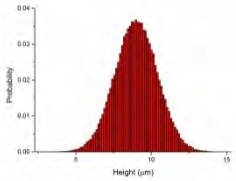
1st shift step	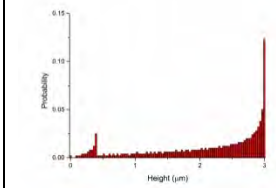	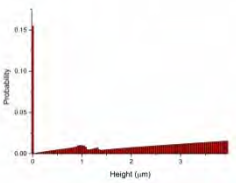	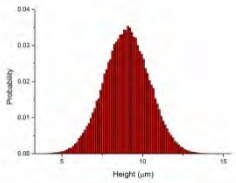
2nd shift step	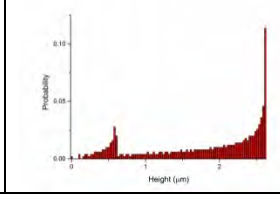	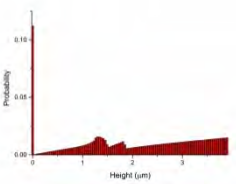	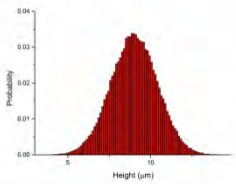

3rd shift step	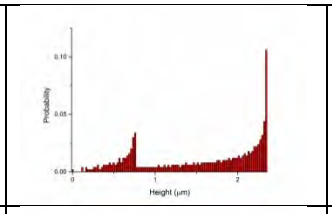	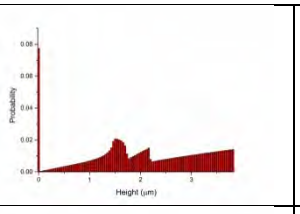	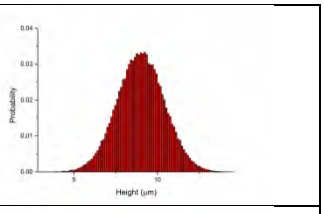
4th shift step	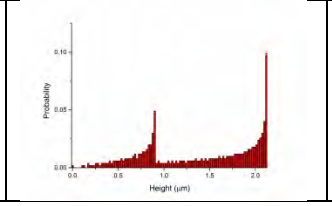	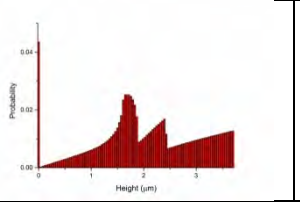	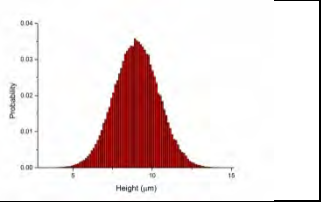

Supplementary Figure S9 (a) Two layer device structures under the condition of lateral sliding; (b)The height distribution of different surface profiles in their original state and side sliding steps of two contact surfaces

Stability performance comparison between different surface profiles and working principles

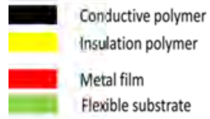 Conductive polymer Insulation polymer Metal film Flexible substrate	 Capacitive type device	 Contact type device	 Contact &Piezoresistive type device
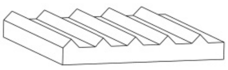	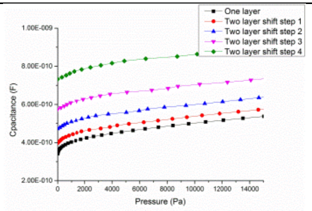	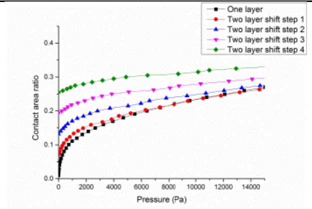	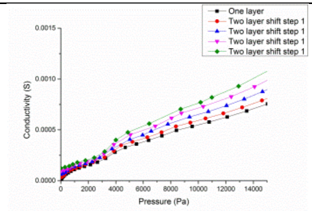
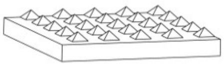	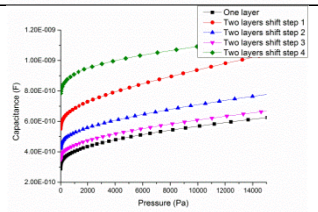	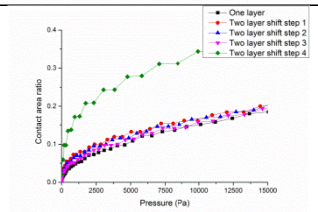	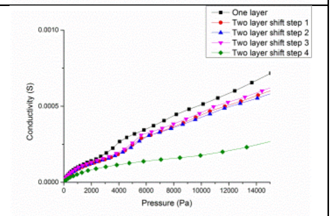
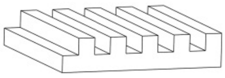	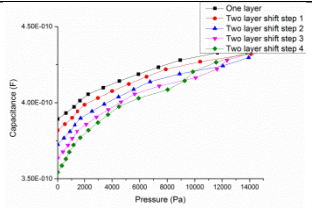	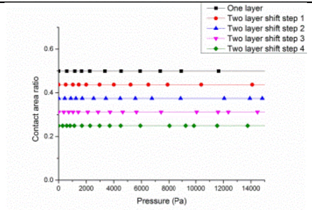	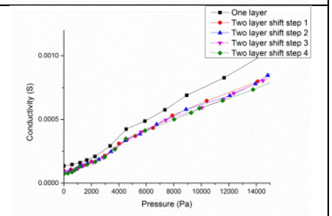
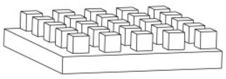	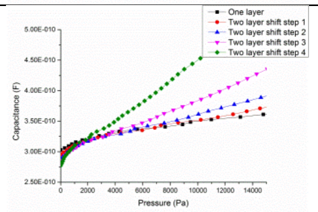	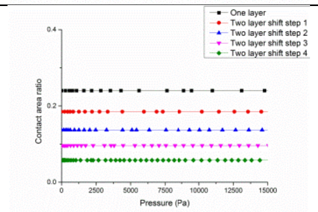	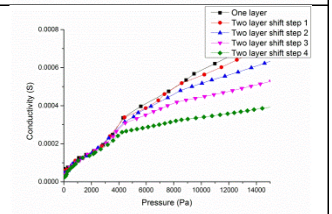
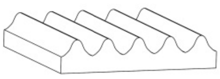	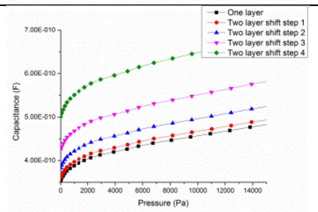	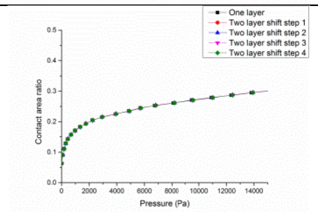	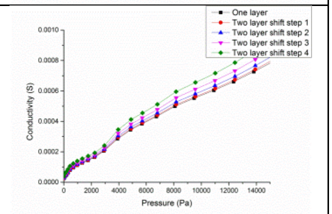
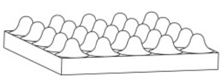	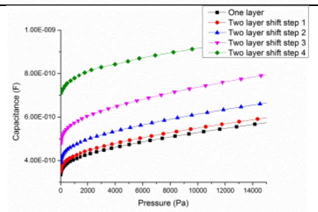	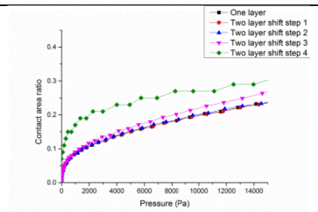	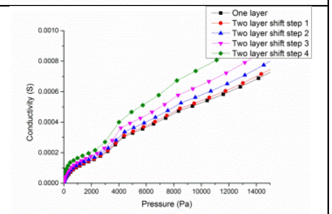
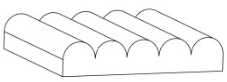	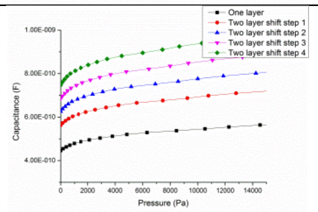	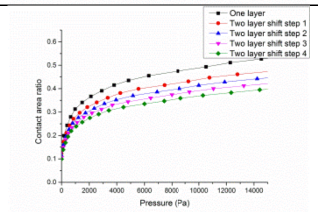	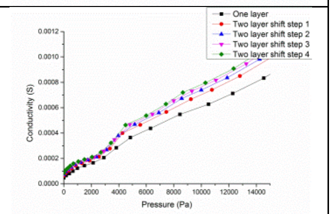

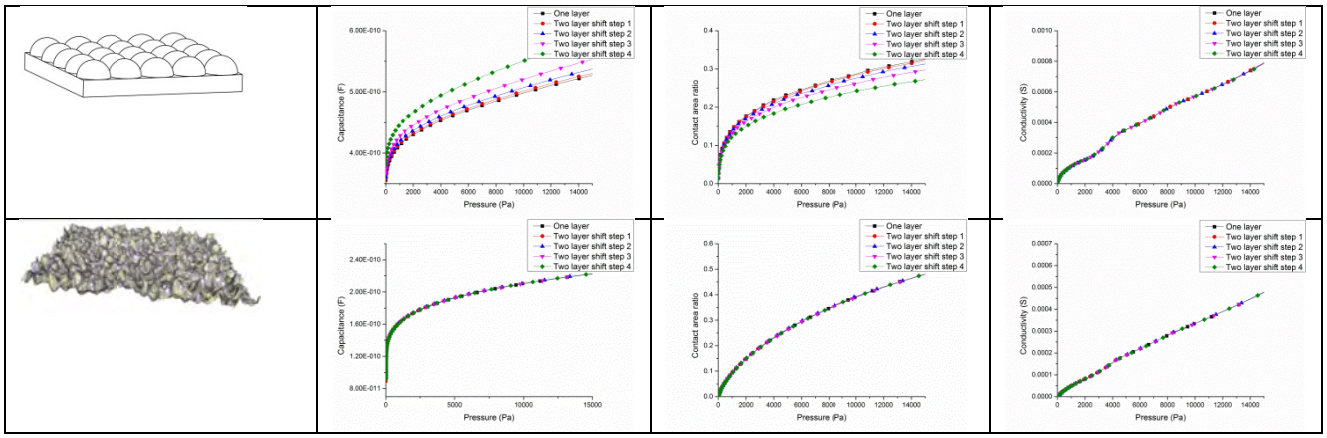

Supplementary Figure S10 To investigate whether the two layer face to face structure have a stable performance when tangential shifts between two surface take place, numerical simulation is carried out at 4 shift steps with interval of $\lambda/4$ along the cross-section direction for 1D profile and diagonal direction for 2D profile. There are also calculated initial performance data for comparison. 9 different surface profiles and 3 working principles are included in this simulation.

The comparison betwen different profiles with pressure mappings and conductance mappings

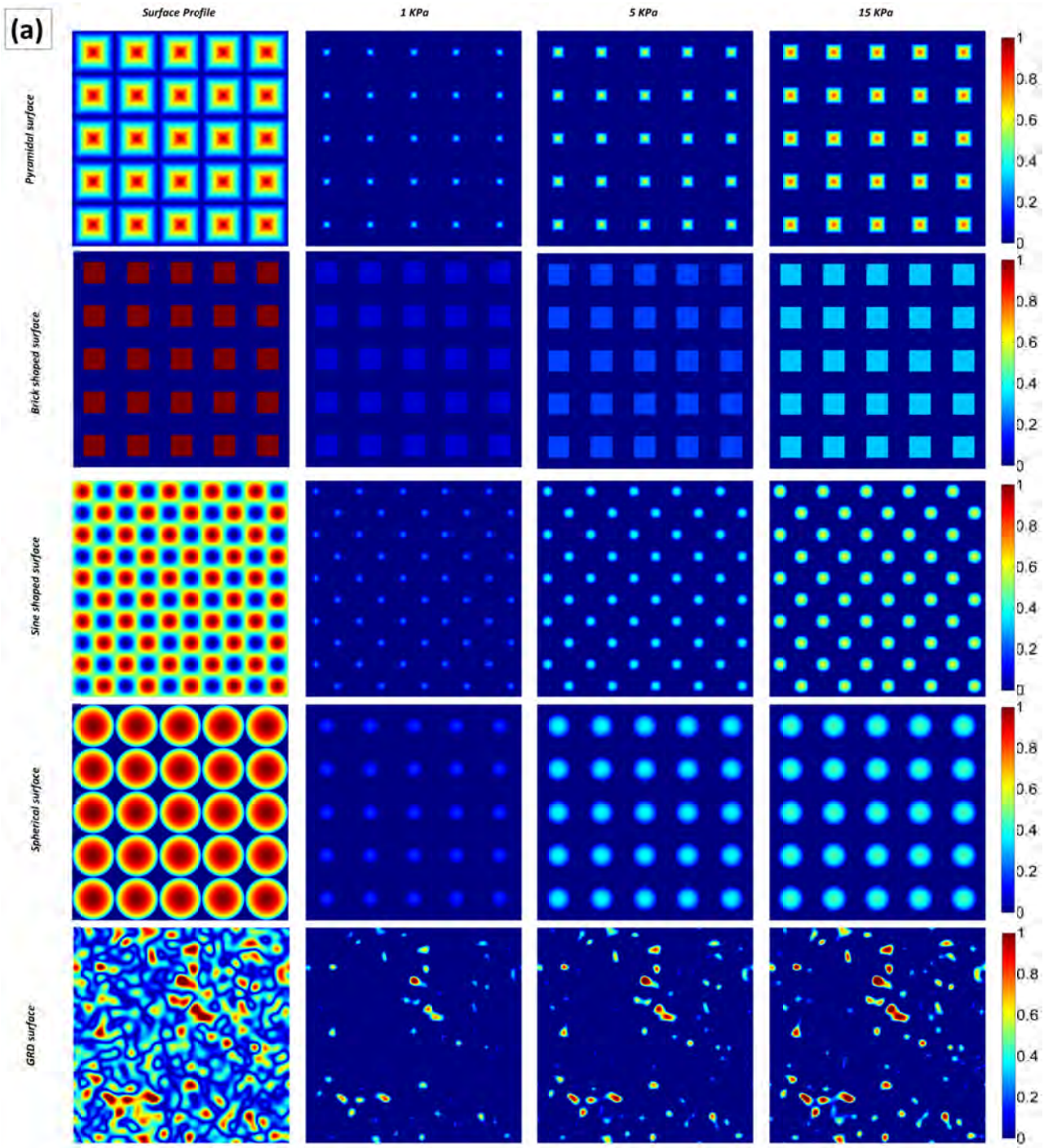

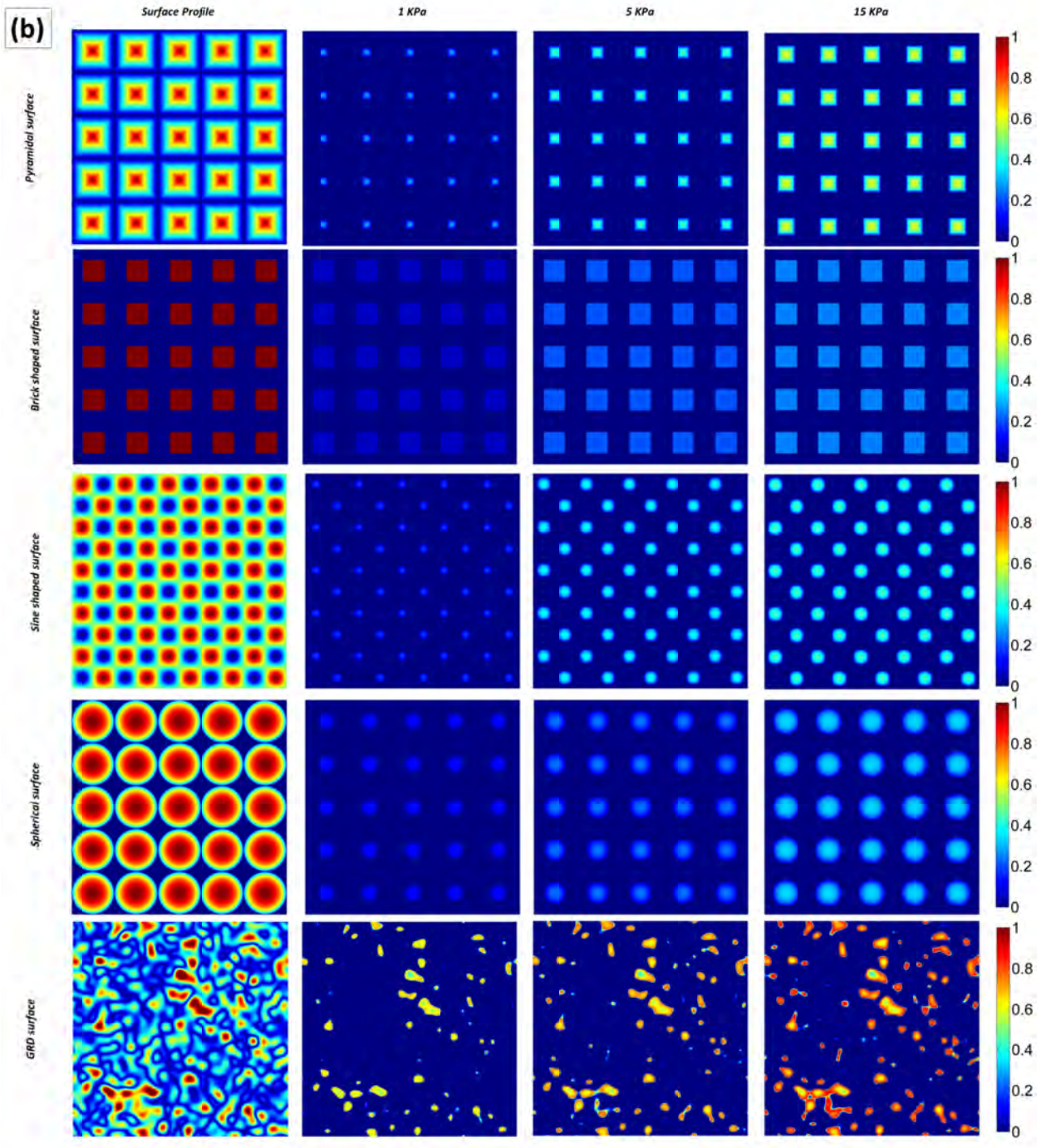

Supplementary Figure S11 The comparison betwen different profiles with (a)pressure mappings and (b)conductance mappings at different pressure levels.

The simulated performance comparison between surface profiles

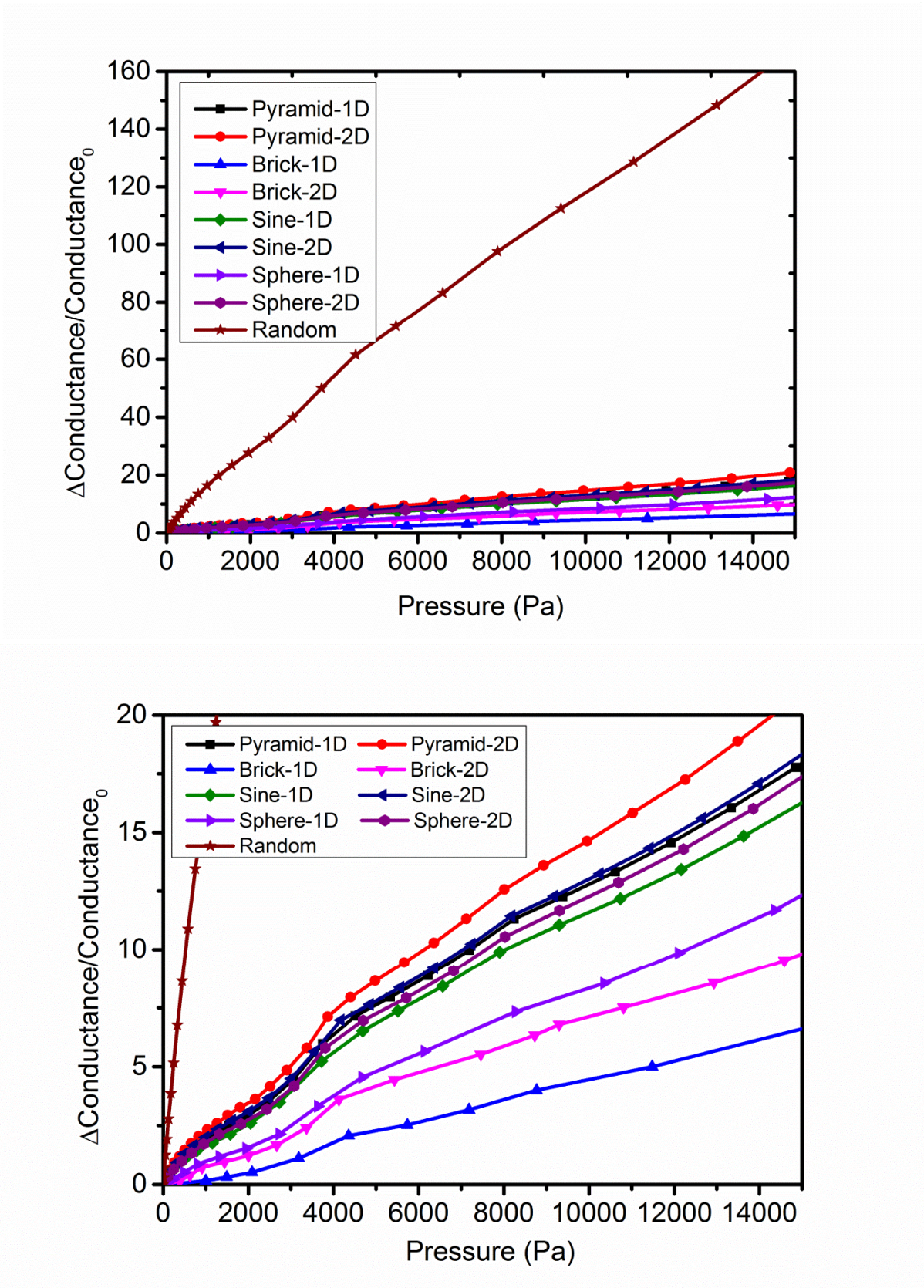

Supplementary Figure S12 The simulated performance comparison between surface profiles (a)Overall plot (b)Magnified plot.